International Journal of Chronic Obstructive Pulmonary Disease

Dovepress
Taylor & Francis Group

Open Access Full Text Article

ORIGINAL RESEARCH

Potential Benefits of Gut Microbiota Modulation in Chronic Obstructive Pulmonary Disease

Jing Li[1], Huilu Zhang[2], Peng Zhang[3], Jie Hu[1]

[1]Department of Pulmonary Medicine, Shanghai Geriatric Medical Center, Shanghai, People's Republic of China; [2]Department of Digestive Diseases of Huashan Hospital, Fudan University, Shanghai, People's Republic of China; [3]Department of Respiratory Disease and Critical Care Medicine, Shanghai Public Health Clinical Center, Fudan University, Shanghai, People's Republic of China

Correspondence: Jie Hu, Department of Pulmonary Medicine, Shanghai Geriatric Medical Center, No. 2560, Chunshen Road, Minhang District, Shanghai, 201104, People's Republic of China, Tel +86 21 51371990, Email hu.jie@zsgmc.sh.cn

Background: The gut-lung axis is increasingly recognized. This study aimed to find out whether and how the gut microbiome involved in the pathogenesis of chronic obstructive pulmonary disease (COPD).

Methods: Gut microbiota was characterized via 16S rRNA gene sequencing in COPD patients and a smoking-induced mouse model. Gut dysbiosis was induced by antibiotic cocktail (ABX) and restored by fecal microbiota transplantation (FMT). Plasma metabolomics was conducted using liquid chromatography-mass spectrometry (LC-MS), and pathway analysis was performed with MetaboAnalyst 5.0. Differentially expressed genes were identified by RNA sequencing and functionally interpreted through gene set enrichment analysis (GSEA).

Results: Both COPD patients and mice showed altered gut microbiota, characterized by a unique microbial composition and reduced diversity. ABX induced gut dysbiosis exacerbated pathological lung changes, impaired lung function, and promoted Treg cell exhaustion in COPD mice. Restoration of gut homeostasis via FMT attenuated these alterations. Higher plasma levels of acetylcholine (ACh) were observed in COPD mice, while the highest ACh levels were found in ABX treated COPD mice compared to controls. Notably, ACh levels correlated positively with genus *Parasutterella*, which was more abundant in COPD mice, and inversely with genera *Candidatus* Saccharimonas and *Lactobacillus*, which were predominant in control mice. Metabolomic pathways analysis revealed enrichment in unsaturated fatty acids biosynthesis and purine metabolism in COPD mice relative to controls.

Conclusion: These findings highlight the involvement of the gut microbiome in COPD development and suggest that maintaining gut homeostasis may represent a novel therapeutic strategy for COPD.

Keywords: COPD, gut, metabolomics, microbiome

Background

Chronic obstructive pulmonary disease (COPD) is a progressive inflammatory disease characterized by irreversible airflow limitation and diverse pulmonary pathological changes, leading to hypoxemia and hypercapnia.[1] Accumulating evidence, including our previous work, indicates that COPD represents a complex multi-component disorder.[2–6] Growing studies have revealed distinct gut microbiota composition and metabolome in COPD patients compared with healthy individuals, suggesting potential cross-talk between gut microbiome and lung.[7–9] As the largest microbial community in the human body, the gut microbiome plays a fundamental role in the development of immune system and maintaining tissue homeostasis. Alterations in its composition and function, termed dysbiosis, have been increasingly implicated in pulmonary disease pathogenesis. A recent report has described that an abnormal gut microbiome is associated with airway inflammation and disease progression in mouse model of COPD.[10] On the other hand, accumulating evidences have supported that COPD patients have increased incidence of gastrointestinal disturbances, such as inflammatory bowel disease and irritable bowel syndrome.[11,12] Despite these observations, the role of "gut-lung axis" in COPD and the precise mechanisms by which the gut microbiome influences disease progression remain incompletely elucidated.

https://doi.org/10.2147/COPD.S594405
Received: 6 February 2026
Accepted: 18 April 2026
Published: 5 May 2026

The gut microbiota plays a critical role not only in food digestion but also in the synthesis and metabolism of nutrients and other bioactive compounds vital for host health. Metabolites derived from the gut microbiota, such as fatty acids, bile acids, vitamins, and amino acids, can enter systemic circulation and contribute to the regulation of metabolic and immune homeostasis.[13] Yet, whether and how the gut microbiota influence plasma metabolomics profile in COPD remains unknown.

Imbalances of immune system and abnormal inflammatory response play an essential role in the pathogenesis of COPD. Damage to airway epithelial cells induced by smoking promotes the release of chemokines and cytokines, initiating innate immune responses and leading to T cells activation and uncontrolled inflammation response, which ultimately drives disease progression.[14] In recent years, accumulating evidences have indicated that gut microbial components and metabolites can modulate local and systemic immunity, thereby influencing the development of pulmonary diseases.[15–17] But whether and how the gut microbiota and its metabolites are involved in regulating immune response and pathogenesis of COPD are still obscure.

Given the emerging significance of the "gut-lung axis" in COPD, the present work aimed to investigate the involvement of the gut microbiome in disease mechanisms. We identified the alterations of gut microbiome in both COPD patients and smoking-induced mouse model and verified disruption of gut homeostasis exacerbated pathological deterioration, lung function decline, and immune imbalance, while restoration of gut homeostasis ameliorated these changes. Furthermore, we found that specific gut microbiota including *Parasutterella, Candidatus* Saccharimonas and *Lactobacillus* could modulate circulating metabolites such as ACh, and thereby shape pulmonary immune responses via regulating Treg cells in the lungs. Taken together, our findings not only delineate a functional connection between the gut microbiome, host metabolism, and pulmonary immunity but also propose novel therapeutic strategies targeting gut microbiota for the treatment of COPD.

Methods

Subject Recruitment

Eight COPD patients and seven healthy control subjects participated in the present study. The COPD patients came from the Shanghai Geriatric Medical Center and the healthy control subjects came from the same residential area. The diagnosis of COPD was made according to the Global Initiative for Chronic Obstructive Lung Disease (GOLD) 2024 guidelines (with post bronchodilator $FEV_1/FVC<70\%$ and $FEV_1<80\%$ predicted).[1] All COPD patients were receiving stable maintenance therapy with long-acting beta-agonists and/or long-acting muscarinic antagonists. Participants were excluded if they had experienced respiratory tract infection, or received treatment with an antibiotic or corticosteroid in the previous 4 weeks, or had a diagnosis of cancer, diabetes, gastrointestinal diseases, asthma, liver or renal dysfunction. All subjects provided written informed consent, and ethics approval was obtained from the Shanghai Geriatric Medical Center (Ethical approval number: ZCLY2025-039). The study was conducted in accordance with the principles of the Declaration of Helsinki.

Samples Collection and Sequencing

Fresh stool samples were obtained from participants by providing them with sterile containers. Samples were then snap-frozen in dry ice and stored at −80°Cuntil processing. Total bacterial DNA was extracted from samples using Magen Hipure Soil DNA kit (Lot: HD150300) according to the manufacturer's instructions. The DNA concentration was quantified using a Qubit® dsDNA HS Assay Kit (Lot: 7E322J9) and a Qubit Fluorometer (Thermo Scientific, Waltham, MA, United States). The extracted DNA from each sample was used as a template to amplify the V3 and V4 hypervariable region of 16S rRNA genes using PCR. The V3 and V4 regions were amplified using forward primer 5′-CCTACGGRRBGCASCAGKVRVGAAT-3′ and reverse primer 5′-GGACTACNVGGGTWTCTAATCC-3′. All libraries were sequenced by using an Illumina MiSeq platform (Illumina, San Diego, CA, USA).

16S rRNA Gene Sequencing Analysis

The forward and reverse reads obtained from double-end sequencing were first concatenated pairwise, and then the concatenated results were filtered for sequences containing N while retaining sequences with a length greater than 200 bp. After quality filtering and removal of chimeric sequences, the final sequences were subjected to OTU clustering using

VSEARCH (1.9.6) with a sequence similarity of 97%. Then, the reference database SILVA was used for sequence alignment. RDP classifier (Ribosomal Database Program) Bayesian algorithm was used to perform species taxonomic analysis on representative sequences of OTU, then the community composition of each sample at different species classification levels was calculated. Based on OTU analysis results, the method of randomly flattening the sample sequence is used to calculate the alpha diversity indices (Chao1 index and Shannon index). Beta diversity was assessed using the Brary-Curtis dissimilarity index calculated from a weighted matrix abundance and visualized by principal co-ordinates analysis (PCoA). Microbial composition differences between groups at each hierarchical level were assessed by linear discriminant analysis effect size (LEfSE) analysis.

Mouse Model of COPD

Six- to eight-week-old male C57BL/6J mice were used in the experiments. Animals were purchased from Shanghai Laboratory Animal Center (China) and were housed in a specific pathogen-free facility. Mice were exposed to cigarette smoke twice per day, five times per week, for eight weeks using a custom-designed smoke-exposure system.[18,19] Each exposure lasted 75 minutes. All protocols used in this study were approved by the Animal Welfare and Ethics Committee of the Department of Laboratory Animal Science, Fudan University (Approval No. 2021JS Huashan Hospital-104). All experiments were performed in accordance with the Guide for the Care and Use of Laboratory Animals published by the National Academy of Sciences. Euthanasia was performed on all mice at the end of experiment. The specific method was as follows: an overdose of pentobarbital sodium solution (concentration: 3%, dosage: 60 mg/kg) was administered via intraperitoneal injection. Following injection, each mouse was placed individually in a warm cage lined with bedding until the complete cessation of breathing and the loss of corneal reflex were confirmed. Subsequently, the death of mice was immediately confirmed by visual verification of cardiac arrest through thoracotomy. The entire euthanasia procedure was conducted in strict accordance with the recommendations for laboratory rodents outlined in the American Veterinary Medical Association (AVMA) guidelines for euthanasia of animals to minimize the suffering of mice.

Antibiotics and Fecal Microbiota Transplantation (FMT) Administration

For antibiotics administration, mice were given an antibiotic cocktail (ABX) consisted of ampicillin (33.2 mg), metronidazole (33.2 mg), neomycin (33.2 mg), and vancomycin (16.7 mg) once a day for 5 days via oral gavage. After the 5th day of oral gavage, ABX were added to the drinking water at a concentration of 1g/L each for ampicillin, metronidazole, and neomycin, and 0.5g/L for vancomycin to deplete gut microbiota as described previously.[20] Mice were maintained on ABX or water for duration of the experiment. For FMT treatment, fresh feces from donor mice (control group mice) were pooled and homogenized in sterile PBS with a final concentration of 100 mg/mL. Then, samples were vortexed and centrifuged (5 minutes, 600×g) and 200 μL of the fecal supernatant was given to mice by oral gavage once a day during the experiment. A total of six mice per experimental subgroup were subjected to 16S rRNA gene sequencing, whereas three mice per group were included for metabolomic analysis.

Pulmonary Function Tests

The mice were anaesthetized via intraperitoneal injection of 4% chloral hydrate. Then a plastic cannula was inserted into mouse trachea and connected to the Animal Lung Function Test System (Shanghai Tawang Intelligent Technology Co., Shanghai, China) to test the pulmonary function. The pulmonary function parameters were obtained using this system include minute ventilation volume (MV), peak expiratory flow (PEF), expiratory flow at 50% tidal volume (EF_{50}), forced expiratory volume in 0.1 s ($FEV_{0.1}$) and forced vital capacity (FVC). Each test was performed at least three times.

Histological Analysis

The fresh lung tissue was fixed in a 10% formaldehyde solution for 24 hours and then embedded in paraffin. Four-micrometre thick sections were stained with hematoxylin and eosin (H&E) and then observed under a light microscope (Nikon eclipse Ti-U, Tokyo, Japan). To assess airspace enlargement, the mean linear intercept (MLI) was measured as a standard parameter. A grid of parallel lines spaced 200μm apart was overlaid, and the total number of intersections

between the grid lines and alveolar septa was manually counted. The MLI was calculated as the total grid length divided by the number of intercepts. All measurements were performed by an observer blinded to the experimental groups.

Detection of Cytokines

Bronchoalveolar lavage was performed with 2 mL of PBS four times to collect the bronchoalveolar lavage fluid (BALF). The returned lavage fluid was then centrifuged at 800×g for 10 minutes at 4°C, and the supernatant was stored at −80°C until used. The levels of interleukin-1β (IL-1β), IL-17, and tumor necrosis factor-α (TNF-α) in BALF were measured using mouse enzyme-linked immunosorbent assay (ELISA) kit according to the manufacturer's instructions (R&D, Minneapolis, MN, USA).

Flow Cytometry Analysis

The left lung was harvested and minced, digested, passed through a 70μm cell strainer, washed twice with ice-cold PBS at 300×g for 5 minutes, and then resuspended in PBS. The single-cell suspension obtained from lung samples were stained for T cells subsets with anti-mouse specific antibodies (included anti-CD3, anti-CD4, anti-CD8, anti-IFN-γ, anti-IL-4, anti-IL-17A, anti-FoxP3) conjugated with either PE, APC, FITC, AmCyan, APC-Cy7, PerCP-Cy5.5, Pacific Blue, PE-Cy7, or Alexa Fluor 700 (BD Biosciences or Thermo Fisher Scientific). In brief, cell surface staining was performed using antibodies against CD3, CD4, or CD8 directly conjugated to APC-Cy7, FITC, or PerCP-Cy5.5 according to standard procedures. For intracellular staining, cells were fixed in BD Fixation/Permeabilization buffer for 40 minutes and washed in BD Permeabilization/Wash buffer, and then incubated with antibodies against with IFN-γ, IL-4, IL-17A, or FoxP3 conjugated with Pacific Blue, PE-Cy7, APC, or PE according to the manufacture's protocol. Flow cytometry was performed on a BD FACS Canto II flow cytometry (BD, Bioscience, San Jose, USA) and analyzed using FlowJo software (Tree Star Inc., Ashland, OR, USA).

RNA-Seq Analysis

Total RNA was extracted from lung tissues using TRIzol Reagent (Invitrogen, Carlsbad, CA, USA) according to the manufacturer's protocol, and analyzed for RNA quantification and quality control using NanoDrop ND2000 (Thermo Fisher Scientific). The RNA samples were sequenced using the NovaSeq 6000 platform (Illumina, San Diego, CA, USA). Libraries were generated using the Truseq RNA sample preparation kit (Illumina). The differentially expressed genes (DEGs) were analyzed using DESeq2 software. The DEGs were prepared according to the following criteria: absolute Log_2 fold change (FC) ≥1 and p adjust < 0.05. For the visualization of the DEGs, volcano plot was generated using the software R 3.2.1.

Liquid Chromatography-Mass Spectrometry (LC-MS) Analysis

After incubation with ice-cold methanol, plasma samples were centrifuged at 12000 rpm for 15 minutes at 4°C, and the supernatants were collected and then placed in −40°C for 1 h. Samples were re-suspended with 2-Chloro-L-phenylalanine prior to the injections on the LC-MS instrument. Metabolites were analyzed by LC-MS in positive and negative ionization modes. Metabolic profiles in samples were determined using the TripleTOF 5600+ platform (AB Sciex). Chromatographic separation of metabolites was performed using an ACQUITY UPLC HSS T3 column (2.1×100 mm, 1.8 μm). The solvent flow rate was 0.3 mL/min, column temperature was 40°C and sample temperature was 4°C. The raw LC-MS data was first converted into ABF format files using software AbfConverter 4.0.0, and then peak detection, peak alignment, peak filtering, and molecular annotation were out using software MS-DIAL. The final standardized data matrix was imported into software SIMCA-P14.0 (Umetrics AB, Umea, Sweden) for multivariate statistical analysis.

Bioinformatic Analysis

Correlation analysis between metabolomic and microbiomic data was undertaken using metabolites and microbiota identified as significantly different between COPD and control mice. Pearson's correlation was calculated using "corr.

test" function within R package psych V2.3.9. The correlation matrix was produced using "pheatmap" function with R package pheatmap v1.0.12.

To determine whether the DEGs were involved in hallmark pathway, gene set enrichment analysis (GSEA) was carried out using the software GSEA4.2.3 (Broad Institute, Cambridge, MA, USA). The normal *p* value and normalized enrichment score (NES) were used to sort the pathways enriched in each group.

Metabolic enrichment analysis and pathway analysis were performed with MetaboAnalyst 5.0 (https://www.metaboanalyst.ca/). Metabolic pathways with adjusted *p* values < 0.05 were considered significantly enrichment.

Statistical Analysis

Data were presented as mean±SD. Multiple comparisons were performed by using one-way ANOVA with the Tukey post-test. Categorical variables were compared using a Chi-squared test. Differences between two groups were evaluated using Student-*t* test or Mann–Whitney test. Mouse survival was calculated using the Kaplan–Meier method and the Log rank test. Statistical analysis was performed with software R 3.2.1 and Graphpad Prism 8. *P* values of <0.05 were considered significant.

Results

Demographic Characteristics of the Participants

The demographic and clinical features of the study participants are summarized in Table 1. A total of 8 COPD patients and 7 healthy controls were enrolled after diagnosis and exclusion criteria. The COPD patients and control cohorts had comparable demographic characteristics with respect to age, sex, BMI, and smoking status ($p>0.05$). As expected, COPD group had lower FEV_1, FVC, and FEV_1/FVC values than those in the control group ($p<0.001$).

Alterations of Gut Microbiome in COPD Patients

To assess overall differences in gut microbial diversity and composition between COPD patients and healthy controls, microbial DNA was extracted from fecal samples and subjected to 16S rRNA gene sequencing. Alpha diversity analysis revealed a significant reduction in COPD patients, as reflected by the Chao 1 ($p=0.046$) and Shannon ($p=0.025$) indices (Figure 1A and B). Furthermore, beta diversity analysis demonstrated a clear separation between the two groups, with the first principal component accounting for 27.2% of the total variance (Figure 1C).

Subsequent analysis focused on alterations in gut microbiota composition between COPD patients and healthy controls. At phylum level, the gut microbiota of both groups contained four major bacterial phyla: Firmicutes, Bacteroidetes, Proteobacteria, and Actinobacteria (Figure 1D and Additional Table S1). At genus level, *Bacteroides* was the most abundance, followed by *Faecalibacterium, Escherichia-Shigella, Subdoligranulum*, and *Blautia* in the cohort overall (Figure 1E and Additional Table S2). To illustrate the taxonomic hierarchy from phylum to genus, the relationships between these levels were visualized using Sankey diagrams (Figure 1F and G), in which the flow width represents relative abundance. Additionally, linear discriminant analysis (LDA) score with LEfSe analysis identified several differentially abundant taxa between the two groups. At the phylum level, Proteobacteria was enriched in COPD patients, while Firmicutes was more abundant in controls. Furthermore, four genera (*Escherichia-Shigella, Bacteroides, Ruminococcus gnavus*, and *Lactobacillus*) exhibited higher relative abundance in COPD patients, while nine genera (*Faecalibacterium, Roseburia, Prevotella-9, Agathobacter, Subdoligranulum, Anaerostipes, Lachnospiraceae_NK4A136, Coprococcus-3*, and *Alistipes*) were more prevalent in healthy controls (Figure 1H).

Alterations of Gut Microbiome in Smoking-Induced COPD Mouse Model

Next, we assessed the gut microbial diversity in smoking-induced COPD mice and found a distinct separation in beta diversity between the COPD and control groups (Figure 2A). At the phylum level, the gut microbiota in both groups was predominantly composed of five major phyla: Firmicutes, Bacteroidetes, Proteobacteria, Verrucomicrobia, and Epsilonbacteraeota (Figure 2B and Additional Table S3). At the genus level, *Lactobacillus* was the most abundance, followed by *Muribaculaceae_Unclassified, Lachnospiraceae_Unclassified, Lachnospiraceae_NK4A136* and

Table 1 Demographic Characteristics of the Study Population

Characteristics	Control Group (n=7)	COPD Group (n=8)	*p* value
Age, years	62.57 ± 9.43	66.38 ± 9.32	0.45
Female/males, n	3/4	3/5	0.99
BMI, kg/m^2	23.94 ± 2.72	24.08 ± 2.84	0.92
Smoking status, n (%)			0.87
Never smoked	4 (57.14)	4 (50.00)	
Current smoker	2 (28.57)	2 (25.00)	
Exsmoker	1 (14.29)	2 (25.00)	
Cigarettes smoked, pack-years			
Current smoker	36.00 ± 4.24	42.50 ± 6.36	0.35
Exsmoker	21.00	20.00 ± 4.24	NA
Comorbidities, n (%)			NA
Hypertension	0 (0)	1 (12.50)	
Cardiovascular disease	0 (0)	2 (25.00)	
Hyperlipidemia	0 (0)	0 (0)	
Dietary habits, n (%)			0.99
High-fat/meat preference	2 (28.57)	2 (25.00)	
Vegetable/fruit preference	5 (71.43)	6 (75.00)	
FEV_1, % predicted	107.5 ± 9.86	46.14 ± 12.84	< 0.001
FVC, % predicted	98.73 ± 8.44	55.87 ± 13.49	< 0.001
FEV_1/FVC	90.58 ± 5.41	49.85 ± 8.29	< 0.001

Notes: Data are presented as mean ± SD, except where indicated otherwise. Differences were evaluated using Student-*t* test or Chi-square test (or Fisher's exact test).
Abbreviations: BMI, body mass index; FEV_1, forced expiratory volume in 1s; FVC, forced vital capacity; NA, not applicable.

Desulfovibrio (Figure 2C and Additional Table S4). To further delineate the phylum-to-genus relationships, Sankey diagrams were constructed (Figure 2D and E). These diagrams explicitly map each bacterial genus to its respective phylum, where the width of each flow is proportional to the relative abundance.

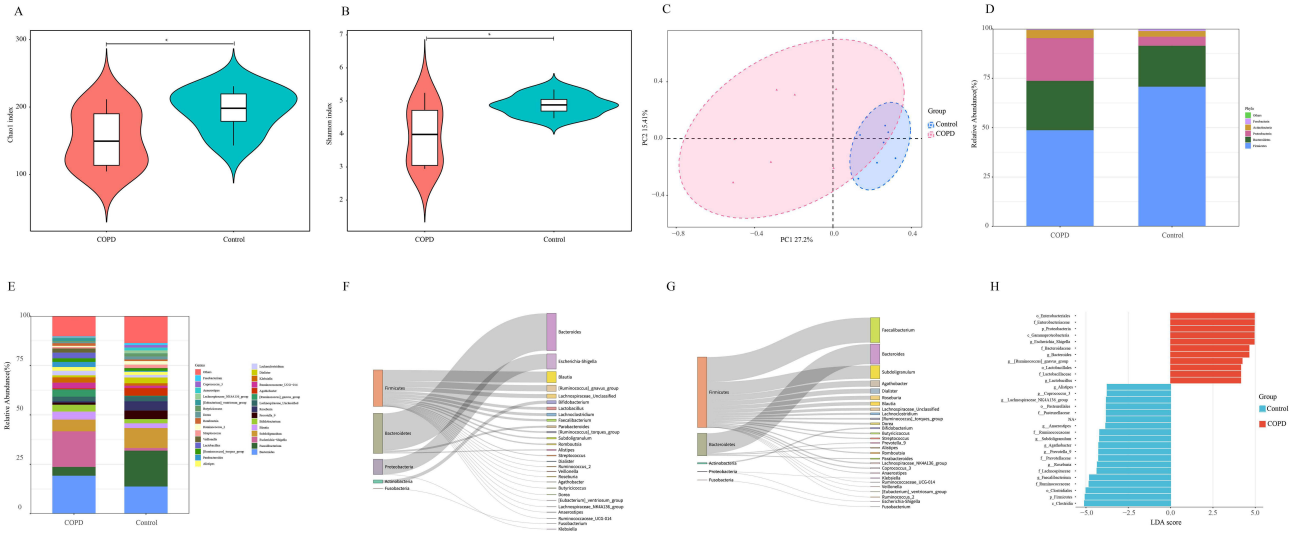

Figure 1 Alterations of gut microbiome in COPD patients. (**A** and **B**) The alpha diversity (Chao 1 index and Shannon index) of the COPD patients (n=8) and healthy control (n=7) (* p<0.05). (**C**) Principal coordinates analysis (PCoA) for gut microbiome taxonomic profile of the two groups. (**D**) The phylum level taxonomic profiles of the gut microbiome of the two groups. Phyla with mean relative abundance <1% are combined into the "other" category. (**E**) The genus level taxonomic profiles of the gut microbiome of the two groups. The top 30 most abundant genera are shown. (**F** and **G**) Sankey diagram of phylum-to-genus relationships in COPD patients and healthy control. Left nodes represent bacterial phyla, and right nodes represent genera. The width of each connecting flow is proportional to the relative abundance of the corresponding genus within each phylum. (**F**) COPD patients; (**G**) healthy controls. (**H**) Linear discriminant analysis (LDA) scores obtained from LEfSe analysis. An LDA effect size of more than 2 was indicate statistically significant differences.

https://doi.org/10.2147/COPD.S594405

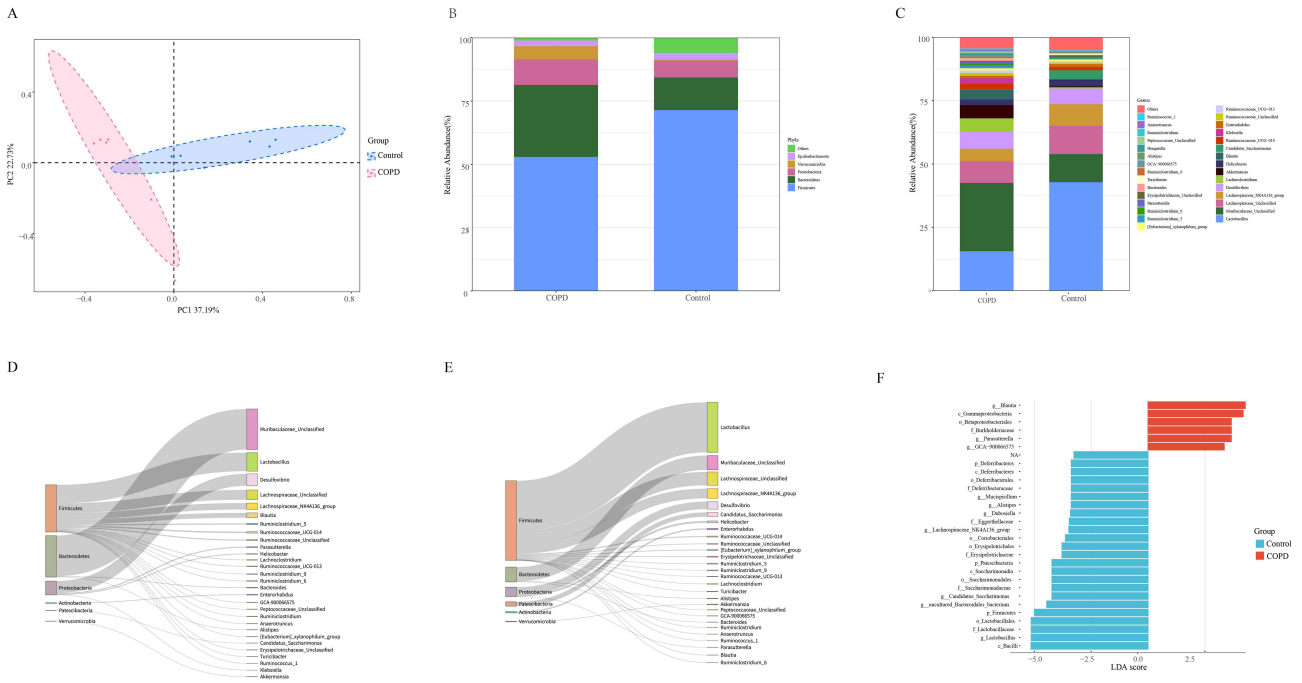

Figure 2 Alterations of gut microbiome in smoking-induced COPD mice. (**A**) The beta diversity (PCoA analysis) of the COPD mice and the control mice (n=6). (**B**) The phylum level taxonomic profiles of the gut microbiome of the two groups. (**C**) The genus level taxonomic profiles of the gut microbiome of the two groups. The top 30 most abundant genera are shown. (**D** and **E**) Sankey diagram of phylum-to-genus relationships in COPD mice and control mice. Left nodes represent bacterial phyla, and right nodes represent genera. The width of each connecting flow is proportional to the relative abundance of the corresponding genus within each phylum. (**D**) COPD mice; (**E**) control mice. (**F**) LDA scores obtained from LEfSe analysis of the two group.

We then compared gut microbial composition between the COPD and control mice. LDA scores identified several differentially enriched taxa: the genera *Blautia* and *Parasutterella* were significantly more abundant in COPD mice, whereas the phyla Firmicutes, Patescibacteria, and Deferribacteres, along with the genera *Lactobacillus, uncultured Bacteroidales bacterium, Candidatus* Saccharimonas, *Lachnospiraceae_NK4A136, Dubosiella, Alistipes*, and *Mucispirillum* were markedly enriched in control animals (Figure 2F).

Disruption of Gut Homeostasis Promoted the Development of COPD

As the alterations of gut microbiome occurred in both COPD patients and mouse model, we then investigated whether disruption of gut homeostasis promoted the development of COPD. To test this hypothesis, we evaluated the effects of antibiotic-induced gut dysbiosis in a smoking-induced mouse model of COPD. As expected, alpha diversity indices were markedly reduced following ABX treatment (Figure 3A and B). Histological examination of H&E stained lung sections from smoking-induced COPD mice revealed characteristic structural abnormalities, including irregular alveolar space enlargement and rupture, leukocyte infiltration, and alveolar wall thickening. The mean linear intercept (MLI), a standard parameter for assessing airspace enlargement, was measured in all groups. The MLI was significantly increased in the COPD group compared with the control group. Moreover, the ABX treated COPD group exhibited a further significant increase in MLI relative to the COPD group (Figure 3M). Notably, ABX treatment exacerbated these pathological changes, leading to more severe alveolar space expansion and rupture, enhanced inflammatory infiltration, and even alveolar hemorrhage (Figure 3C–F). In line with the histopathological findings, ABX administration increased mortality (Figure 3G) and accelerated lung function decline in COPD mice, as reflected by reduced MV, PEF, EF_{50}, and a lower $FEV_{0.1}$/FVC ratio (Figure 3I–L). Additionally, BALF concentrations of the proinflammatory cytokines (IL-1β, TNF-α, and IL-17) were substantially elevated in COPD group, and ABX administration further amplified this inflammatory response (Figure 3H). Collectively, these findings demonstrate that gut dysbiosis exacerbates disease progression in COPD.

https://doi.org/10.2147/COPD.S594405

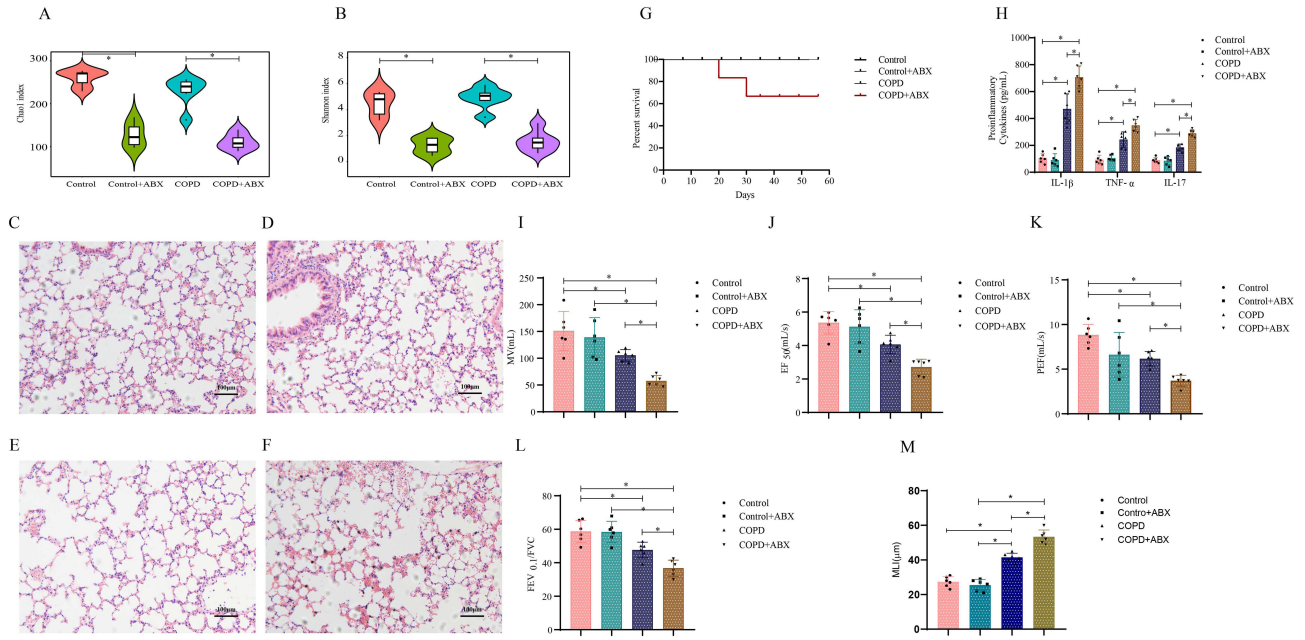

Figure 3 Gut dysbiosis promoted the development of COPD. (**A** and **B**) The alpha diversity (Chao 1 index and Shannon index) in control group, ABX treated control group, COPD group, and ABX treated CODP group (n=6) (* p<0.05). (**C**–**F**): Representative HE staining image of lung sections in control group (C) ABX treated control group (D) COPD group (E) and ABX treated COPD group (F). (**G**) Mortality of mice in the four groups. Survival was recorded for 8 weeks. (**H**) Levels of proinflammatory cytokines (IL-1β, TNF-α, and IL-17) in BALF in different groups (* p<0.05). (**I**–**L**): Lung function was measured on 8 weeks in the four groups (* p<0.05). (**M**) Mean linear intercept (MLI) values in different groups (* p<0.05).

Gut Microbiome Influenced Plasma Metabolome in COPD Mouse Model

The gut microbiota has been found to have the capability to influence host metabolomic profiles. To identify metabolites potentially involved in the gut microbiota mediated regulation of COPD, plasma metabolites were examined by LC-MS in COPD mouse model. Comparative analysis revealed significantly elevated levels of acetylcholine (ACh) and 3-indoxyl sulfate (I3S), along with reduced levels of gamma-glutamylleucine, kynurenine, acetylcarnitine, arachidonic acid, docosahexanoic acid, eicosapentaenoic acid, xanthine, and hypoxanthine in COPD mice relative to controls (Figure 4A). To functionally interpret these changes, we carried out metabolites set enrichment and pathway analysis using MetaboAnalyst 5.0. Enrichment analysis highlighted significant accumulation of metabolites unsaturated fatty acids, butyrophenones, indoles, and xanthines (p<0.05; Figure 4B), while pathway analysis indicated involvement of the biosynthesis of unsaturated fatty acids and purine metabolism (p<0.05; Figure 4C).

Notably, compared with the COPD group, ABX treated COPD mice exhibited markedly elevated levels of ACh, hexanoyl-L-carnitine, lysine, D-alloisoleucine, and citric acid, whereas levels of serotonin, 3-indolepropionic acid, hippuric acid, and para-cresol were remarkably reduced (Figure 4A). Enrichment analysis revealed significant accumulation of serotonins, indolyl carboxylic acids, TCA acids, short-chain acyl carnitines, and amino acids (p<0.05; Figure 4D). Corresponding pathway analysis identified phenylalanine metabolism and biotin metabolism as the most prominently altered pathways (p<0.05; Figure 4E).

According to the aforementioned results, we generated a correlation heatmap to visualize associations between gut microbial genera and plasma metabolites in control and COPD mice, aiming to further elucidate the role of the gut microbiome in COPD pathogenesis (Figure 4F). Among the microbiota examined, *Parasutterella, Bacteroides, and Candidatus* Saccharimonas showed the strongest associations with plasma metabolites. Specifically, the levels of ACh and I3S exhibited positive correlation with the abundance of *Parasutterella*, but negative correlations with *Candidatus* Saccharimonas, and *Lactobacillus*. The levels of kynurenine, xanthine, and hypoxanthine correlated positively with *Candidatus* Saccharimonas and negatively with *Bacteroides*. These observations suggest that the gut microbiome may influence COPD progression through metabolite-mediated mechanisms.

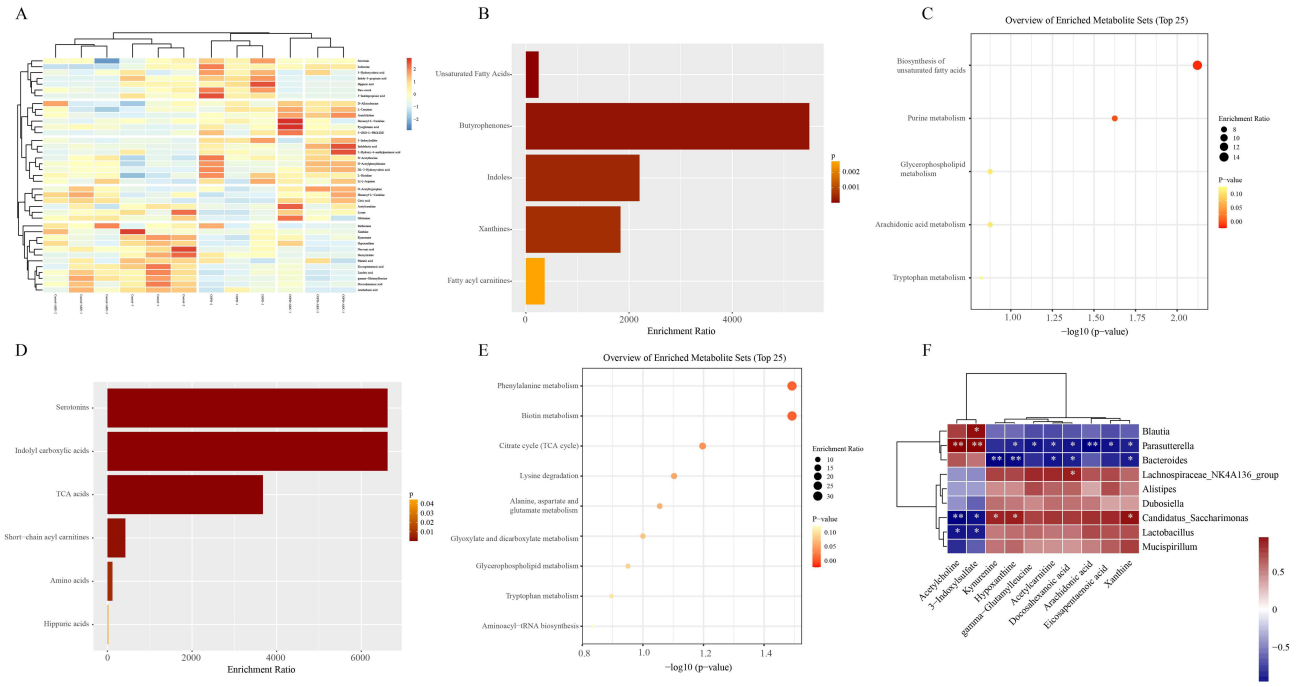

Figure 4 Gut microbiome influenced plasma metabolomic profile in COPD mouse model. (**A**) Heatmap of the plasma metabolomic profile in control group, ABX treated control group, COPD group, and ABX treated CODP group (n=3). (**B**) The enrichment analysis of the differentially expressed plasma metabolites between COPD mice and control mice. (**C**) The pathway analysis of the differentially expressed plasma metabolites between COPD mice and control mice. (**D**) The enrichment analysis of the differentially expressed plasma metabolites between COPD mice and ABX treated COPD mice. (**E**) The pathway analysis of the differentially expressed plasma metabolites between COPD mice and ABX treated COPD mice. (**F**) Correlation analysis between discriminatory gut microbial genera and plasma metabolites. Red denotes positive correlation; blue denotes negative correlation. Color bar represents Pearson's correlation coefficients. Correlation scores were visualized with gradient colors by using the ggplot2 package of R. Significant correlations denoted by white star (* $p<0.05$, ** $p<0.01$).

Gut Dysbiosis Induced Imbalance of Immune System in COPD Mouse Model

Since ABX treatment exacerbated pathological changes, lung function decline, inflammation, and mortality in COPD mice in our vivo experiment, we then performed RNA sequencing to compare transcriptional profiles between COPD and ABX treated COPD groups and explore the underlying mechanisms. The RNA-seq results displayed that the gene expression profiles of the two groups were markedly distinct (Figure 5A). To functionally characterize the differentially expressed genes (DEGs) associated with ABX exposure, we performed GSEA to identify biologically relevant pathways. GSEA indicated significant enrichment of gene sets related to abnormal tissue metabolite concentration, the citric acid TCA cycle and respiratory electron transport, fatty acid metabolism, hypoxia, lung CD4 naive T cell, TGF-β signaling and KRAS signaling pathway in ABX treated COPD mice (Figure 5B).

Considering the critical role of immune dysregulation in COPD pathogenesis, we analyzed immune cell subpopulations in the lungs of different experimental groups using flow cytometry. While the frequencies of Th1 cells, Th2 cells, and Th17 cells remained comparable across groups, a significant reduction in Treg cells was observed in COPD mice compared with controls. Notably, this reduction was further exacerbated in ABX treated COPD mice (Figure 5C–G). These findings suggest that gut dysbiosis contributes to pulmonary immune imbalance in COPD, particularly through the suppression of Treg populations.

Gut Microbiome Restoration Prevented the Development of COPD

To confirm the protective potential of gut homeostasis in COPD, we administered FMT from healthy control mice to COPD mice via daily oral gavage for eight weeks. As expected, FMT treated COPD mice exhibited a marked reduction in both inflammatory cell infiltration (Figure 6A–D) and MLI (Figure 6E) relative to the untreated COPD group. This suggests that FMT significantly attenuated lung pathological injury in COPD mice. Consistent with histological improvement, FMT treated COPD mice exhibited better lung function, reflected by higher MV, PEF, EF_{50}, and $FEV_{0.1}$ /FVC ratio compared to untreated COPD animals (Figure 6F). At the immune level, FMT restored the pulmonary

 https://doi.org/10.2147/COPD.S594405

https://doi.org/10.2147/COPD.S594405

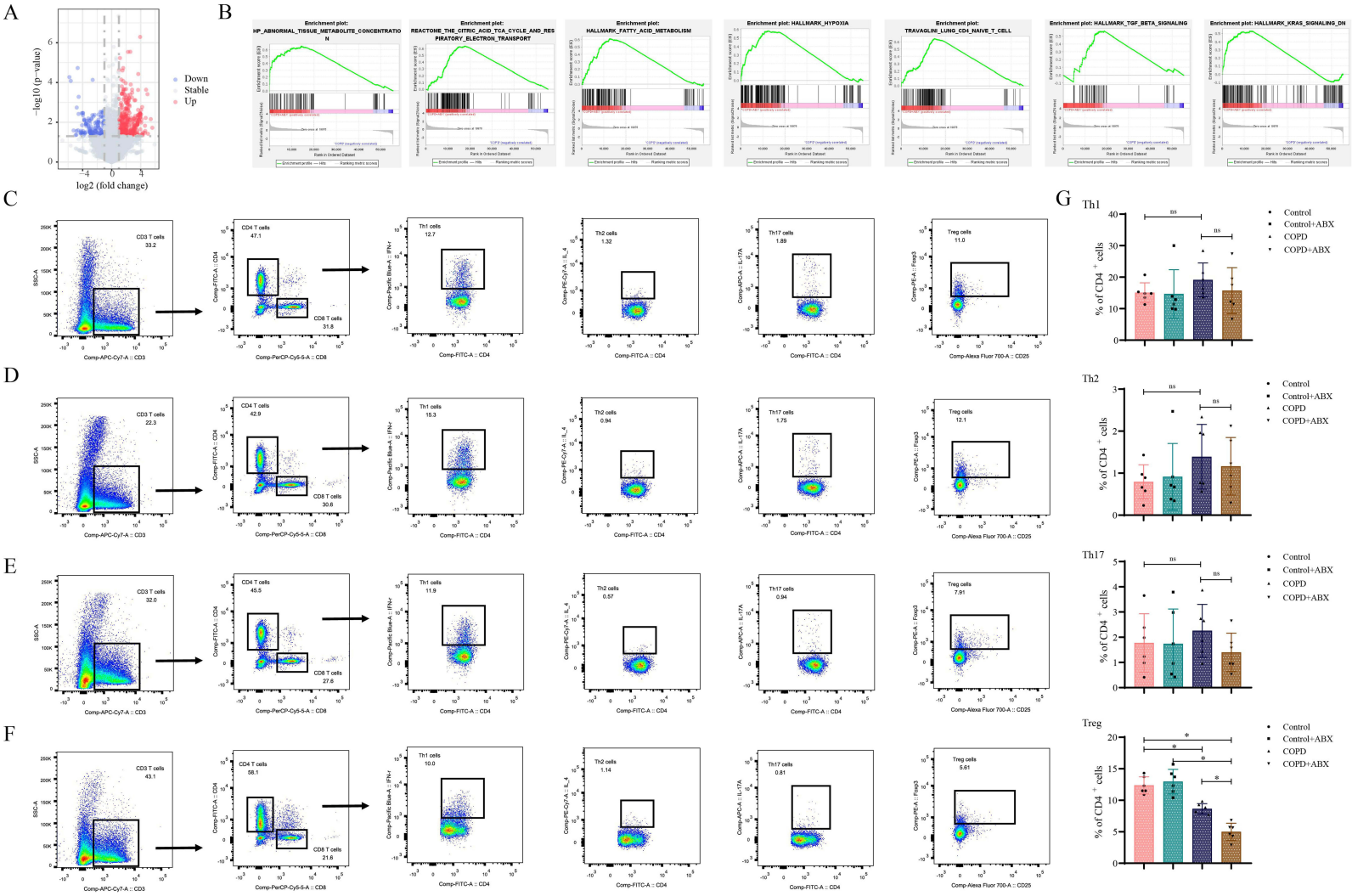

Figure 5 Gut dysbiosis induced imbalance of immune system in COPD mouse model. (**A**) The differentially expressed genes (DEGs) of lung tissues between COPD mice and ABX treated COPD mice were illustrated by volcano plot. (**B**) Signaling pathway enrichment analysis using DEGs by GSEA. (**C**–**F**): The subsets of T cells in lungs were examined by flow cytometry in control group (C) ABX treated control group (D) COPD group (E) and ABX treated CODP group (F). The right arrow indicates that the cells within the gated region were further subdivided into subpopulations (CD4+T cells, Th1 cells, Th2 cells, Th17 cells, and Treg cells). (**G**) Statistical analysis of the Th1 cells, Th2 cells, Th17 cells, and Treg cells in the four groups (* $p<0.05$, ns indicates not significant).

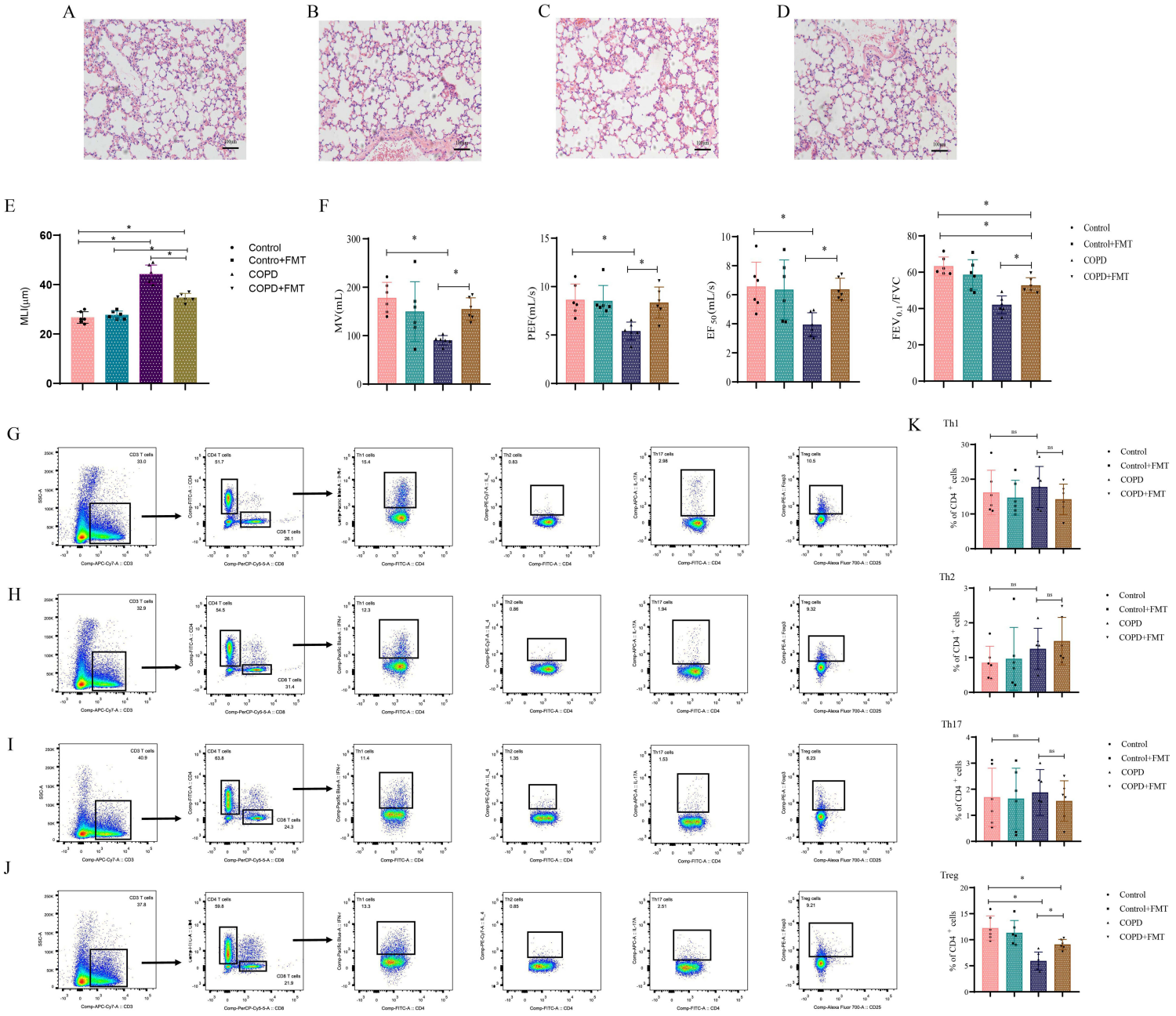

Figure 6 Restoration of gut homeostasis by FMT prevented the development of COPD. (**A**–**D**): Representative HE staining image of lung sections in control group (A) FMT treated control group (B) COPD group (C) and FMT treated CODP group (D) (n=6). (**E**) Mean linear intercept (MLI) values in different groups (* p<0.05). (**F**) Lung function was measured in the four groups (* p<0.05). (**G**–**J**): The subsets of T cells in lungs were examined by flow cytometry in control group (G) FMT treated control group (H) COPD group (I), and FMT treated CODP group (J). The right arrow indicates that the cells within the gated region were further subdivided into subpopulations (CD4+T cells, Th1 cells, Th2 cells, Th17 cells, and Treg cells). (**K**) Statistical analysis of the Th1 cells, Th2 cells, Th17 cells, and Treg cells in the four groups (* p<0.05, ns indicates not significant).

frequency of Treg cells in COPD mice, whereas the proportions of Th1 cells, Th2 cells, and Th17 cells remained unaltered between the two groups (Figure 6G–K). These results demonstrate that reestablishing gut homeostasis through FMT mitigates COPD progression, potentially through selective restoration of immunoregulatory Treg cells populations in the lung.

Discussion

In this study, we demonstrate a substantial influence of the gut microbiome on COPD pathogenesis. We observed distinct alterations in both gut microbial composition and plasma metabolomic profiles in COPD models. ABX-inducted gut dysbiosis significantly increased mortality, exacerbated pathological lung injury, accelerated lung function decline, and promoted immune dysregulation. Conversely, restoration of gut homeostasis via FMT ameliorated these impairments in COPD mouse model. ACh levels were elevated in COPD mice and further increased in ABX-treated animals. Notably, ACh abundance correlated positively with *Parasutterella*, which was more abundant in COPD mice, but negatively with *Candidatus* Saccharimonas and *Lactobacillus*, which were predominant in control mice. Plasma metabolomic analysis revealed enrichment of the biosynthesis of unsaturated fatty acids and purine metabolism in COPD mice compared with controls. Moreover, phenylalanine metabolism and biotin metabolism were enriched in ABX-treated COPD mice relative to the COPD group.

Numerous experimental and epidemiological evidences have highlighted the important and complex cross-talk between the gut microbiome and the lungs, referred to as the "gut-lung axis".[21] Gut microbial dysbiosis, usually characterized by reduced bacterial diversity or altered community composition, has been implicated in the pathogenesis of several respiratory diseases, including asthma, COPD, lung cancer, and respiratory infection.[15] Although previous studies have reported alterations in specific gut bacterial taxa in COPD patients, findings have inconsistent.[10,22] In this study, we analyzed the gut microbiome composition in a cohort of COPD patients and confirmed that the dominant phyla were Firmicutes, Bacteroidetes, Proteobacteria, and Actinobacteria, which consistent with earlier reports.[10] Further analysis at the genus level, an area of notable discrepancy across previous studies,[10,22] revealed that our COPD cohort exhibited increased abundances of *Escherichia-Shigella, Bacteroides, Ruminococcus gnavus*, and *Lactobacillus*, alongside decreased abundances of *Faecalibacterium, Roseburia, Prevotella-9, Agathobacter, Subdoligranulum, Anaerostipes, Lachnospiraceae, Coprococcus-3*, and *Alistipes*. Discrepancies between our findings and those of previous studies may be attributed to several factors. First, differences in dietary habits, geographical regions, and the inherent heterogeneity of COPD may all contribute to the observed variability. Second, methodological variations, such as the use of different fecal DNA extraction kits and variations in extraction efficiency, may lead to differential lysis of bacterial cells and thus shape the microbial profiles obtained. Finally, differences in clinical characteristics across study populations, such as COPD severity and comorbidity prevalence, also serve as important sources of variation across studies. Moreover, we observed a significant reduction in alpha-diversity, which reflects microbial diversity within each sample and distinct clustering in beta-diversity, which indicates structural differences in microbial communities between COPD patients and controls. Given these findings, gut microbiome composition is significantly altered in COPD patients. In addition to the gut microbiome, accumulating evidence indicates that the lung microbiome is also significant altered in COPD. Compared with healthy individuals, COPD patients show increased abundance of Proteobacteria and reduced microbial diversity in the lower airways.[23] These changes have been associated with disease severity, exacerbation frequency, and inflammatory responses. Although our study focused on the gut microbiome, future studies should investigate the potential crosstalk between the gut and lung microbiomes in COPD.

In order to reveal whether and how the gut microbiome involved in the development of COPD, we employed smoking-induced mouse model of COPD. The overall structure of the gut microbiota in COPD mice was similar to that observed in human patients, with Firmicutes, Bacteroidetes, Proteobacteria, Verrucomicrobia, and Epsilonbacteraeota constituting the dominant phyla. At the genus level, COPD mice exhibited significantly increased abundances of *Blautia* and *Parasutterella*, along with decreased levels of *Lactobacillus, Bacteroidales, Candidatus* Saccharimonas, *Lachnospiraceae_NK4A136, Dubosiella, Alistipes*, and *Mucispirillum* compared with controls. While some genus-level differences between human and mouse microbiota likely reflect host species specificity, these findings consistently demonstrate the changes in the gut microbiome of COPD. We next investigate the functional contribution of gut

microbiota to COPD by inducing gut dysbiosis via ABX administration in the mouse model. ABX-mediated disruption of gut homeostasis increased mortality, exacerbated pulmonary pathology including inflammation, emphysema, and alveolar hemorrhage and accelerated lung function decline. Importantly, restoration of gut homeostasis by FTM from healthy control mice dramatically mitigated both lung structural damage and functional impairment. These experimental findings highlight the importance of gut microbiome homeostasis in COPD development and suggest that microbial modulation may represent a promising therapeutic strategy for treating or preventing COPD.

Metabolomic studies have indicated that dysregulation of amino acid metabolism, lipid metabolism, and energy production pathways were involved in the development of COPD.[24] Gut microbiota contributes to host physiology in part through the production of small molecule metabolites that accumulate in systemic circulation.[25,26] Emerging metabolomic analysis thus offers a valuable strategy to elucidate how gut microbial activity influences COPD. In the present study, we analyzed the differences of plasma metabolomic profile in mice and found significantly elevated levels of ACh and I3S, along with reduced levels of gamma-glutamyl-leucine, kynurenine, acetylcarnitine, arachidonic acid, docosahexanoic acid, eicosapentaenoic acid, xanthine, and hypoxanthine in COPD group relative to controls. Enrichment analysis identified unsaturated fatty acids, butyrophenones, indoles, and xanthines were enriched. Furthermore, ABX treated COPD mice exhibited increased levels of ACh, hexanoyl-L-carnitine, lysine, D-alloisoleucine, and citric acid, but decreased levels of serotonin, 3-indolepropionic acid, hippuric acid, and para-cresol compared with untreated COPD mice, with corresponding enrichment in serotonins, indolyl carboxylic acids, TCA acids, short-chain acyl carnitines, and amino acid. Notably, the level of ACh was elevated in COPD mice and further increased following ABX treatment. ACh, as a primary parasympathetic neurotransmitter in the airways, released from cholinergic nerve terminals and airway cells not only regulates airway construction and mucus secretion, but also modulates airway inflammation and remodeling.[27] The acetylcholine system participates in the pathogenesis of respiratory diseases, and anticholinergics have long been used in the treatment of COPD. Our findings suggest that ACh as a potential mediator linking the gut microbiome to COPD pathogenesis, either as a contributing factor or a downstream consequence. Yet, the causal relationship between gut microbiota-derived metabolites and COPD progression needs further study.

Metabolic pathway analysis revealed distinct alterations in COPD mice compared with controls, including biosynthesis of unsaturated fatty acids (such as arachidonic acid, docosahexanoic acid, eicosapentaenoic acid) and purine metabolism. These findings align with clinical observations of reduced plasma polyunsaturated fatty acids and altered polyunsaturated fatty acids metabolism in COPD patients.[28,29] Purine metabolism, a key process in energy transfer, generates metabolites like hypoxanthine and xanthine, which have been positively associated with inflammation of COPD.[30] Furthermore, comparison between ABX-treated and untreated COPD mice identified phenylalanine metabolism and biotin metabolism as notably altered pathways, underscoring the potential for gut microbiota to modulate COPD through metabolic pathway. Recently, studies have demonstrated that high level of serum phenylanaine, an essential amino acid, was associated with the severer lung injury and increased mortality of ARDS.[31,32] Moreover, biotin deficiency, which impairs fatty acid, glucose and amino acid metabolism, as well as immune cells function of T cells, B cells, NK cells and dendritic cells, has been shown to exacerbate inflammatory responses.[33,34] These findings supported the evidence of functional crosstalk between the gut microbiome and plasma metabolome in COPD, although the precise underlying mechanisms remain unclear.

To elucidate the mechanisms by which gut microbiome-derived metabolites regulate COPD pathogenesis, we examined potential association between discriminant microbial genera and key plasma metabolite. Notably, *Parasutterella, Bacteroides*, and *Candidatus* Saccharimonas demonstrated the strongest correlations with circulating metabolites. Previous studies have indicated that *Parasutterella*, as a core gut microbiota component, may participate in modulating inflammatory responses and mucosal barrier integrity;[35,36] however, the precise mechanisms underlying its metabolic regulation remain to be fully defined. Of particular interest, ACh level exhibited a positive correlation with *Parasutterella* abundance, but negative correlations with *Candidatus* Saccharimonas, and *Lactobacillus*. Recent studies have reported that certain gut microbiota, including *Lactobacillus plantarum, Bacillus subtilis, Escherichia coli*, and *Staphylococcus aureus*, can synthesize or metabolize neurotransmitters, such as ACh.[37] In our present study, the observed alterations in ACh may reflect direct gut microbial production or indirect host effects mediated through nonneuronal cholinergic system involving airway and immune cell, which need more researches.

https://doi.org/10.2147/COPD.S594405

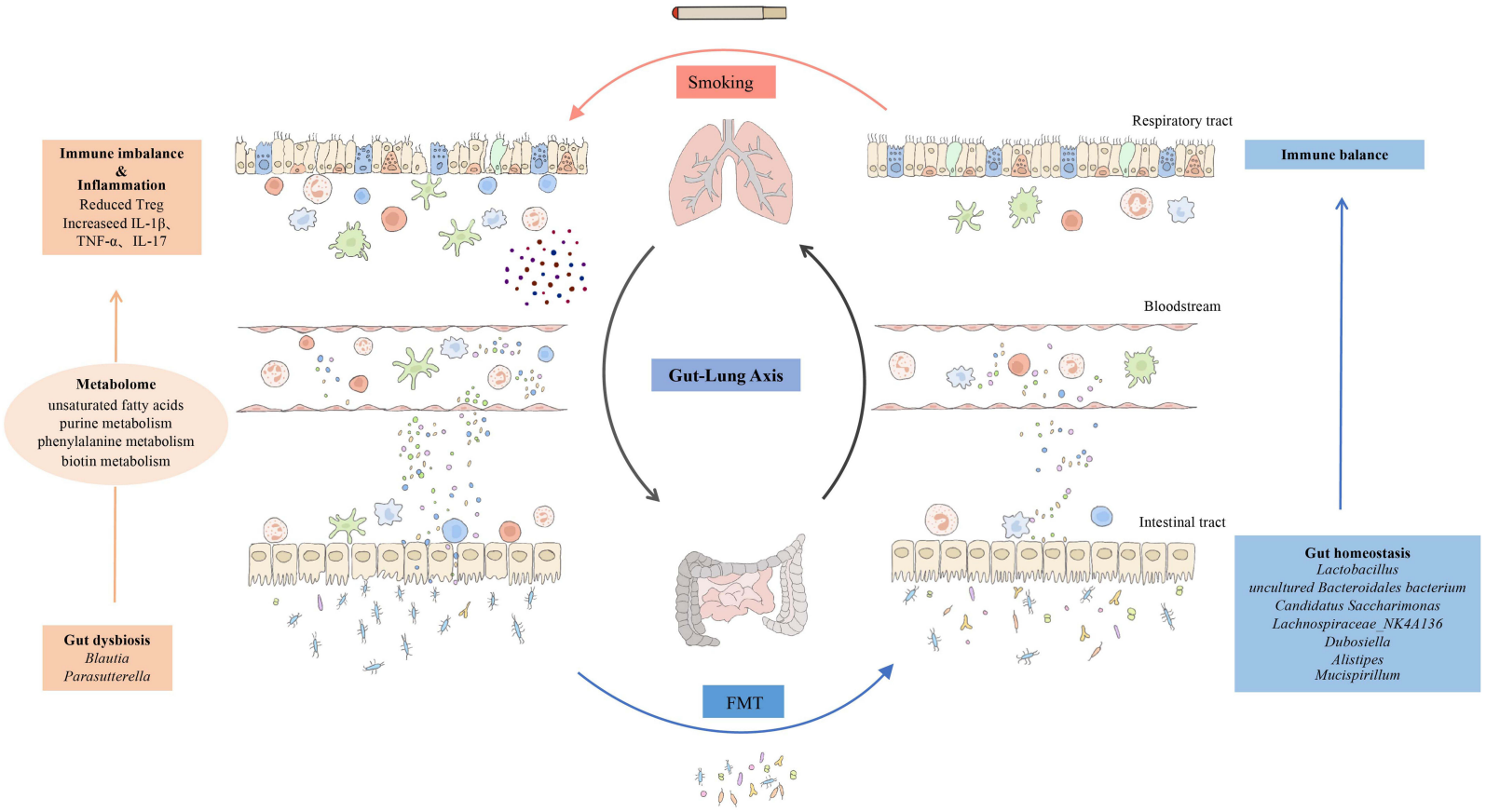

Figure 7 Potential mechanisms by which gut microbiome influences COPD. The imbalance of intestinal flora causes the alterations of plasma metabolites, which further aggravates the immune imbalance and inflammatory response in COPD lungs. FMT, however, can effectively restore the balance of the gut microbiota, which restores the immune system in the lung and inhibits the progression of COPD.

To investigate the mechanisms basis of gut microbiome driven pulmonary effects in COPD, we compared lung gene expression levels between COPD and ABX treated COPD using RNA-seq coupled with bioinformatic analysis. The RNA-seq analysis identified 441 differentially expressed genes (DEGs) between the two groups, among which 118 (26.76%) were downregulated and 323 (73.24%) were upregulated. GSEA analysis revealed significant enrichment of DEGs in pathways related to abnormal tissue metabolite concentration, the citric acid TCA cycle and respiratory electron transport, fatty acid metabolism, hypoxia, lung CD4 naive T cell, TGF-β signaling and KRAS signaling. Given the established role of immune dysregulation in COPD and the known immunomodulatory effects of the gut microbiome, we further analyzed T cells subpopulations in lung tissue based on GSEA results. We observed a significant reduction in the frequency of Treg cells in COPD mice, which was further exacerbated by ABX treatment. Importantly, restoration of gut homeostasis by FMT dramatically restored Treg cell levels in COPD mice. Treg cells are key immunoregulatory cells that suppress autoreactive lymphocytes through a variety of mechanisms, including immunomodulatory cytokines secretion and direct cell-to-cell contact. Dysfunction of Treg cells leads to autoimmune disease and inflammatory disease,[38] and previous studies have reported Treg cell deficiency in COPD patients and animal models.[39,40] Our results demonstrate that modulation of gut homeostasis could restore pulmonary immune balance in COPD, potentially through the recovery of Treg mediated immunoregulation.

This study had several limitations. First, the relatively small cohort size and the absence of analysis correlating gut microbiota composition with COPD severity may limit the generalizability of our findings. While the number of cases will be continuously increased in our future work, we anticipate that our findings will encourage further investigation in this field. Moreover, the 8-week smoke exposure, although standard, does not fully replicate the chronic course of human COPD. Second, the biological functions of the identified key gut microbial taxa and metabolites, particularly their specific roles in COPD pathogenesis, require further experimental characterization. Third, the mechanistic link among gut microbial species, host metabolic pathways and pulmonary pathology remain to be fully elucidated. Fourth, negative extraction or sequencing controls were not included in our study. Although we performed computational decontamination to mitigate potential contamination, physical negative controls should be incorporated in future studies to more rigorously exclude potential reagent or laboratory contamination, as these are known confounders in microbiome sequencing. Fifth, this study is limited by the relative nature of 16S rRNA sequencing data. Unmeasured differences in total bacterial load between groups could influence the interpretation of compositional changes. Future studies should employ qPCR to quantify absolute bacterial load and confirm that the observed compositional shifts are not driven by variations in total microbial biomass. Nonetheless, our results provide preliminarily evidence that gut microbial dysbiosis contributes to COPD progression and that restoration of gut microbiota may be a novel therapeutic strategy for COPD.

Conclusion

Overall, our results highlight the profound impact of gut dysbiosis on COPD development (Figure 7). These findings indicate that maintaining gut homeostasis might be beneficial in attenuating lung function decline, restoring immune system imbalance, and mitigating disease progression in COPD. The therapeutic strategy of anticholinergics, together with other methods of gut microbiota modulation, such as FMT could be beneficial to COPD patients.

Data Sharing Statement

The datasets used and/or analyzed during the current study are available from the corresponding author on reasonable request.

Acknowledgments

The authors thank Yu Gu, Xiaobao Shen, and Manyi Ji for their technical assistance.

Author Contributions

All authors made a significant contribution to the work reported, whether that is in the conception, study design, execution, acquisition of data, analysis and interpretation, or in all these areas; took part in drafting, revising or critically

reviewing the article; gave final approval of the version to be published; have agreed on the journal to which the article has been submitted; and agree to be accountable for all aspects of the work.

Funding

This study was supported by the National Natural Science Foundation of China (No: 81700075).

Disclosure

The authors declare no competing interests.

References

1. Global Initiative for Chronic Obstructive Lung Disease (GOLD). Global strategy for the diagnosis, management, and prevention of chronic obstructive pulmonary disease. Available from: https://goldcopd.org/2024-gold-report/. Accessed April 21, 2026.
2. Li J, Fei GH. The unique alterations of hippocampus and cognitive impairment in chronic obstructive pulmonary disease. *Respir Res*. 2013;14:140. doi:10.1186/1465-9921-14-140
3. Li J, Huang Y, Fei GH. The evaluation of cognitive impairment and relevant factors in patients with chronic obstructive pulmonary disease. *Respiration*. 2013;85:98–105. doi:10.1159/000342970
4. Fabbri LM, Celli BR, Agustí A, et al. COPD and multimorbidity: recognising and addressing a syndemic occurrence. *Lancet Respir Med*. 2023;11:1020–1034.
5. Celli BR, Cote CG, Marin JM, et al. The body-mass index, airflow obstruction, dyspnea, and exercise capacity index in chronic obstructive pulmonary disease. *N Engl J Med*. 2004;350:1005–1012. doi:10.1056/NEJMoa021322
6. Woodruff PG, Agusti A, Roche N, et al. Current concepts in targeting chronic obstructive pulmonary disease pharmacotherapy: making progress towards personalised management. *Lancet*. 2015;385(9979):1789–1798. doi:10.1016/S0140-6736(15)60693-6
7. Bowerman KL, Rehman SF, Vaughan A, et al. Disease-associated gut microbiome and metabolome changes in patients with chronic obstructive pulmonary disease. *Nat Commun*. 2020;11:5886. doi:10.1038/s41467-020-19701-0
8. Lai HC, Lin TL, Chen TW, et al. Gut microbiota modulates COPD pathogenesis: role of anti-inflammatory *Parabacteroides goldsteinii* lipopolysaccharide. *Gut*. 2022;71:309–321. doi:10.1136/gutjnl-2020-322599
9. Qu L, Cheng Q, Wang Y, Mu H, Zhang Y. COPD and gut-lung axis: how microbiota and host inflammasome influence COPD and related therapeutics. *Front Microbiol*. 2022;13:868086. doi:10.3389/fmicb.2022.868086
10. Li N, Dai Z, Wang Z, et al. Gut microbiota dysbiosis contributes to the development of chronic obstructive pulmonary disease. *Respir Res*. 2021;22:274. doi:10.1186/s12931-021-01872-z
11. Raftery AL, Tsantikos E, Harris NL, Hibbs ML. Links between inflammatory bowel disease and chronic obstructive pulmonary disease. *Front Immunol*. 2020;11:2144. doi:10.3389/fimmu.2020.02144
12. Shen Z, Qiu B, Chen L, Zhang Y. Common gastrointestinal diseases and chronic obstructive pulmonary disease risk: a bidirectional Mendelian randomization analysis. *Front Genet*. 2023;14:1256833. doi:10.3389/fgene.2023.1256833
13. Brestoff JR, Artis D. Commensal bacteria at the interface of host metabolism and the immune system. *Nat Immunol*. 2013;14:676–684. doi:10.1038/ni.2640
14. Cosio MG, Saetta M, Agusti A. Immunologic aspects of chronic obstructive pulmonary disease. *N Engl J Med*. 2009;360:2445–2454. doi:10.1056/NEJMra0804752
15. Li CX, Liu HY, Lin YX, Pan JB, Su J. The gut microbiota and respiratory diseases: new evidence. *J Immunol Res*. 2020;2020:2340670. doi:10.1155/2020/2340670
16. Rastogi S, Mohanty S, Sharma S, Tripathi P. Possible role of gut microbes and host's immune response in gut-lung homeostasis. *Front Immunol*. 2022;13:954339. doi:10.3389/fimmu.2022.954339
17. Skelly AN, Sato Y, Kearney S, Honda K. Mining the microbiota for microbial and metabolite-based immunotherapies. *Nat Rev Immunol*. 2019;19:305–323.
18. Beckett EL, Stevens RL, Jarnicki AG, et al. A new short-term mouse model of chronic obstructive pulmonary disease identifies a role for mast cell tryptase in pathogenesis. *J Allergy Clin Immunol*. 2013;131:752–762. doi:10.1016/j.jaci.2012.11.053
19. Brassington K, Chan SM, Seow HJ, et al. Ebselen reduces cigarette smoke-induced endothelial dysfunction in mice. *Br J Pharmacol*. 2021;178:1805–1818. doi:10.1111/bph.15400
20. Li H, Xie J, Guo X, et al. *Bifidobacterium* spp. and their metabolite lactate protect against acute pancreatitis via inhibition of pancreatic and systemic inflammatory responses. *Gut Microbes*. 2022;14:2127456. doi:10.1080/19490976.2022.2127456
21. Wang L, Cai Y, Garssen J, Henricks PAJ, Folkerts G, Braber S. The bidirectional gut-lung axis in chronic obstructive pulmonary disease. *Am J Respir Crit Care Med*. 2023;207:1145–1160. doi:10.1164/rccm.202206-1066TR
22. Liu Y, Teo SM, Méric G, et al. The gut microbiome is a significant risk factor for future chronic lung disease. *J Allergy Clin Immunol*. 2023;151:943–952. doi:10.1016/j.jaci.2022.12.810
23. Monsó E. Microbiome in chronic obstructive pulmonary disease. *Ann Transl Med*. 2017;5:251. doi:10.21037/atm.2017.04.20
24. Ran N, Pang Z, Gu Y, et al. An updated overview of metabolomic profile changes in chronic obstructive pulmonary disease. *Metabolites*. 2019;9:111. doi:10.3390/metabo9060111
25. Nicholson JK, Holmes E, Kinross J, et al. Host-gut microbiota metabolic interactions. *Science*. 2012;336:1262–1267. doi:10.1126/science.1223813
26. Dodd D, Spitzer MH, Van Treuren W, et al. A gut bacterial pathway metabolizes aromatic amino acids into nine circulating metabolites. *Nature*. 2017;551:648–652. doi:10.1038/nature24661
27. Li D, Wu J, Xiong X. The role of the acetylcholine system in common respiratory diseases and COVID-19. *Molecules*. 2023;28:1139. doi:10.3390/molecules28031139

28. Patchen BK, Balte P, Bartz TM, et al. Investigating associations of omega-3 fatty acids, lung function decline, and airway obstruction. *Am J Respir Crit Care Med*. 2023;208:846–857. doi:10.1164/rccm.202301-0074OC
29. Van Der Does AM, Heijink M, Mayboroda OA, et al. Dynamic differences in dietary polyunsaturated fatty acid metabolism in sputum of COPD patients and controls. *Biochim Biophys Acta Mol Cell Biol Lipids*. 2019;1864(3):224–233. doi:10.1016/j.bbalip.2018.11.012
30. Esther CR, Coakley RD, Henderson AG, Zhou YH, Wright FA, Boucher RC. Metabolomic evaluation of neutrophilic airway inflammation in cystic fibrosis. *Chest*. 2015;148:507–515. doi:10.1378/chest.14-1800
31. Viswan A, Ghosh P, Gupta D, Azim A, Sinha N. Distinct metabolic endotype mirroring Acute Respiratory Distress Syndrome (ARDS) subphenotype and its heterogeneous biology. *Sci Rep*. 2019;9:2108. doi:10.1038/s41598-019-39017-4
32. Xu J, Pan T, Qi X, et al. Increased mortality of acute respiratory distress syndrome was associated with high levels of plasma phenylalanine. *Respir Res*. 2020;21:99. doi:10.1186/s12931-020-01364-6
33. Kuroishi T. Regulation of immunological and inflammatory functions by biotin. *Can J Physiol Pharmacol*. 2015;93:1091–1096. doi:10.1139/cjpp-2014-0460
34. Agrawal S, Agrawal A, Said HM. Biotin deficiency enhances the inflammatory response of human dendritic cells. *Am J Physiol Cell Physiol*. 2016;311:C386–C391. doi:10.1152/ajpcell.00141.2016
35. Li R, Li M, Li B, Chen WH, Liu Z. *Cannabis sativa* L. alleviates loperamide-induced constipation by modulating the composition of gut microbiota in mice. *Front Pharmacol*. 2022;13:1033069. doi:10.3389/fphar.2022.1033069
36. Li S, Yang S, Zhang Y, et al. Amino acid-balanced diets improved DSS-induced colitis by alleviating inflammation and regulating gut microbiota. *Eur J Nutr*. 2022;61:3531–3543. doi:10.1007/s00394-022-02906-y
37. Chen Y, Xu J, Chen Y. Regulation of neurotransmitters by the gut microbiota and effects on cognition in neurological disorders. *Nutrients*. 2021;13:2099. doi:10.3390/nu13062099
38. Thomas R, Qiao S, Yang X. Th17/Treg imbalance: implications in lung inflammatory diseases. *Int J Mol Sci*. 2023;24:4865. doi:10.3390/ijms24054865
39. Sileikiene V, Laurinaviciene A, Lesciute-Krilaviciene D, Jurgauskiene L, Malickaite R, Laurinavicius A. Levels of CD4+ CD25+ T regulatory cells in bronchial mucosa and peripheral blood of chronic obstructive pulmonary disease indicate involvement of autoimmunity mechanisms. *Adv Respir Med*. 2019;87:159–166. doi:10.5603/ARM.2019.0023
40. Eriksson Ström J, Pourazar J, Linder R, et al. Airway regulatory T cells are decreased in COPD with a rapid decline in lung function. *Respir Res*. 2020;21:330. doi:10.1186/s12931-020-01593-9